УДК 537.62.64:669.018.6

Nanocrystalline microstructure formation during hydrogen-induced phase transformations in $Nd_2Fe_{14}B$ hard magnetic alloy

S.B. Rybalka

sbrybalka@yandex.ru

Donetsk National Technical University, 58 Artem St., 83000 Donetsk, Ukraine

Формирование нанокристаллической микроструктуры в ходе индуцированных водородом фазовых превращений в магнитотвердом сплаве $Nd_2Fe_{14}B$

Рыбалка С.Б.

Донецкий национальный технический университет, ул. Артема 58, 83000 Донецк, Украина

The kinetics and features of nanocrystalline microstructure formation during direct and reverse hydrogen-induced phase transformations in $Nd_2Fe_{14}B$ alloy has been studied. It has been established that a hydrogen-vacuum treatment carried out in accordance with the kinetic data of transformations in Nd_2Fe_{14} alloy leads to a formation of nanocrystalline homogeneous microstructure with average grains size ~0.3 μm. It is shown that carrying out direct and reverse transformations taking into account of kinetic features of transformations as temperature and transformation time allow to avoid abnormal growth processes a main hard magnetic $Nd_2Fe_{14}B$ phase that is one of the main factors for permanent magnets obtaining with high coercivity without very complicated and expensive of alloying procedures.

Keywords: microstructure; hard magnetic alloys; kinetics; gas-solid reactions; scanning electron microscope.

Исследована кинетика и особенности формирования нанокристаллической микроструктуры при прямом и обратном индуцированных водородом фазовых превращениях в сплаве $Nd_2Fe_{14}B$. Установлено, что водородо-вакуумная обработка, осуществленная в соответствии с кинетическими данными превращений в сплаве $Nd_2Fe_{14}B$, приводит к образованию нанокристаллической гомогенной микроструктуры со средним размером зерен ~0,3 мкм. Показано, что проведение прямого и обратного превращений с учетом кинетических особенностей превращений как температура и время превращения, позволяет предотвратить процессы аномального роста основной магнитотвердой фазы $Nd_2Fe_{14}B$, что является одним из основных факторов для получения постоянных магнитов с высокой коэрцитивной силой без весьма сложных и дорогостоящих процедур легирования.

Ключевые слова: микроструктура; магнитотвердые сплавы; кинетика; газ–твердое тело реакции; сканирующий электронный микроскоп.

1. Introduction

From the point of view of condensed matter physics and metal physics, there is a well known approach to treatment of metals and alloys, based on the establishment of the following relationship: treatment conditions - microstructure features - physical properties [1,2]. In other words, this approach includes the following important stages: (i) investigation of transformation kinetics features during treatment and construction of the isothermal kinetics diagrams, also known as Transformation-Temperature-Time (T-T-T) diagrams; (ii) investigation of the microstructure features at different transformation conditions in accordance with the T-T-T diagrams; (iii) study of the relationship between obtained microstructure and some physical properties of a treated alloy (mechanical, magnetic, etc.). This approach has been successfully applied for treatment of not only metals and steels, but also of the hard magnetic alloys such as $SmCo_5$, Sm_2Fe_{17}, Al-Ni-Co, Co-Cu-Ce and others alloys [3-5].

Nowadays, permanent magnets made of $R_2Fe_{14}B$ (where R means Nd, Er, Pr, Tb, etc.) type alloys possess the best

magnetic properties with maximum magnetic energies (~ 400 kJ/m^3) and extreme values of a coercive force and remanence [6]. The improvement of magnet properties will allow to miniaturize user's final products, and therefore constitutes a significant advance in engineering.

At present, there exist many methods to improve magnetic properties, such as powder metallurgy [7], rapid quenching [8], mechanical alloying [9], hot working [10], sintering, etc. However, these methods have some disadvantages. For instance, magnets produced by the pulverizing a cast ingot and a subsequent sintering do not show sufficient coercivities [11,12].

Recently Takeshita and Nakayama have proposed a new method to improve magnetic properties by the so-called HDDR-process (Hydrogenation-Decomposition-Desorption-Recombination) [13-15] based on hydrogen-induced phase and structural transformations in $Nd_2Fe_{14}B$ type alloys, a new method of hydrogen treatment which is a unique method to produce nanocrystalline powders of the Nd-Fe-B type for permanent magnets with improved magnetic properties [15-19].

From the point of view of the condensed matter physics, the above-mentioned HDDR process is based on the subsequent direct and reverse hydrogen-induced phase transformations [20-23]. Direct hydrogen-induced phase transformation occurs in a hydrogen atmosphere (~ 0.1 MPa) at 600-900°C, as a result of alloy interaction with hydrogen, the initial $Nd_2Fe_{14}B$ alloys decomposes into the following phases [21]:

$$Nd_2Fe_{14}B + H_2 \rightarrow NdH_2 + \alpha\text{-}Fe + Fe_2B \quad (1)$$

Then, the following hydrogen evacuation from the decomposed alloy lead to the reverse hydrogen-induced phase transformation with recombination of the decomposed phases into initial $Nd_2Fe_{14}B$ phase, but having a submicron grains size, in accordance with the following phase scheme [21]:

$$NdH_2 + \alpha\text{-}Fe + Fe_2B \rightarrow Nd_2Fe_{14}B \quad (2)$$

In many cases, the HDDR-processes are based on empirical approaches where the treatment in hydrogen atmosphere and in vacuum is conducted at various temperatures and processing times (from 30 minutes up to 2.6-3 hours in hydrogen and from 30 minutes up to 1 hour in vacuum [13-19]). In some cases, when some of the above-described HDDR schemes are applied to the $Nd_2Fe_{14}B$ type alloys with various chemical compositions, it can lead to an abnormal grains growth in the hard magnetic $Nd_2Fe_{14}B$ Φ-phase and, as a result, the coercivity decrease.

The investigations described in the works [24,25,26] have shown that coercivity of the $Nd_2Fe_{14}B$ permanent magnets is a function the transformation time and temperature during hydrogen-induced transformations in the $Nd_2Fe_{14}B$ type alloy.

On the other hand, as it was shown in our previous works, the HDDR process is based on the hydrogen-induced diffusive phase transformations in solid state and evolution of these transformations strongly depends on the temperature and on the hydrogen pressure [20-23].

In order to optimize magnetic properties, it is necessary to control the reaction rates during hydrogen-induced phase transformations in the $Nd_2Fe_{14}B$ type alloys. Consequently, establishment of the relationship "kinetics of transformations-microstructure-magnetic properties" for the $Nd_2Fe_{14}B$ type alloys is an important problem whose solution will lead to a new, improved HDDR-technology.

Therefore, the main goal of this work is to establish the relationship between the hydrogen-induced phase transformation kinetics and microstructure features of the $Nd_2Fe_{14}B$ alloy.

2. Experimental details

Experiments were performed on original $Nd_2Fe_{14}B$ alloy (CNRS, Grenoble, France) of a nominal composition ($Nd_{15.0}Fe_{77.0}B_{8.0}$ at.%). Alloy was prepared by arc melting in a high pure argon atmosphere and then crushed into powders with a particle size 50-600 μm. Then alloy has been treated by the scheme proposed below in hydrogen atmosphere of 0.1 MPa and vacuum ~ 1 Pa. The treatment procedure was the following: firstly, the $Nd_2Fe_{14}B$ alloys are heated in vacuum up to a desired temperature; then at the same constant temperature the reaction chamber is filled with hydrogen to develop a direct hydrogen induced phase transformation, i.e. decomposition of initial $Nd_2Fe_{14}B$ alloy into NdH_2, Fe_2B and α-phase of Fe. The evolution of phase transformations have been studies with the use of special hydrogen-vacuum

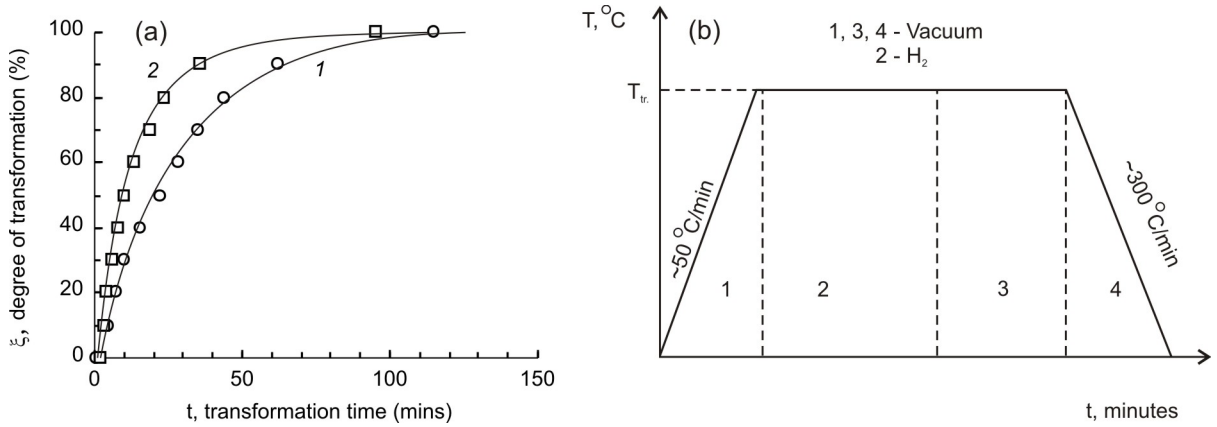

Fig. 1. (a) The kinetic curves for the direct (curve 1) and reverse (curve 2) hydrogen induced phase transformation in $Nd_2Fe_{14}B$ alloy. (b) Experimental procedure for obtaining the $Nd_2Fe_{14}B$ alloy samples for microstructure studies.

equipment with a Sadikov's type magnetometer [20,21]. Afterwards, when the direct transformation is completed, hydrogen is evacuated from the chamber, leading to the development of the reverse hydrogen induced phase transformation, i.e. recombination of the decomposed phases into initial $Nd_2Fe_{14}B$ phase. Finally, when the reverse transformation is completed, the $Nd_2Fe_{14}B$ alloy powder is cooled down to the room temperature in vacuum. The above-mentioned experiments allow to establish the time needed for the direct and reverse phase transformations and to draw the kinetic curves in the coordinates 'degree of transformation-time of transformation' [21]. In particular, the kinetic curves for the direct (curve 1) and reverse (curve 2) phase transformations carried out in hydrogen at pressure of 0.1 MPa and in vacuum ~ 1 Pa at transformation temperature of 730°C are presented in Figure 1a. On the base of the obtained kinetic curves the treatment was carried out for the investigation of the microstructures features.

The scheme of the applied treatment is shown in Figure 1b. In this case, the procedure was the following: firstly, a direct phase transformation in the sample was achieved in accordance with the kinetic data from Figure 1a (region 2 in Figure 2b); then, after the completion of the direct transformation, the reverse transformation was induced by the evacuation of hydrogen from the chamber (region 3 in Figure 2b) before reaching some degree of reverse transformation (20, 50, 80 and 100% in our case) according to the kinetic data from Figure 1a; then $Nd_2Fe_{14}B$ sample was cooled in vacuum with the speed ~300°C/min (region 4 in Figure 2b). Then microstructure investigations were carried out for the samples. The microstructure was studied by using the scanning electron microscope (SEM) JSM T300 with the device for the local analysis Link 860-500. SEM images processing have been performed using special programs for the microanalysis ZAF-4/FSL and SIA.

3. Results and discussion

Figure 2a shows the SEM image of the microstructure of the initial $Nd_2Fe_{14}B$ alloy in secondary electrons mode before the phase transformations. As can be seen from Fig. 2a, microstructure of an initial $Nd_2Fe_{14}B$ alloy has typical dendritic structure with the insufficient magnetic isolation of a $Nd_2Fe_{14}B$ hard magnetic Φ-phase (grey regions in Fig. 2a) by Nd-rich intergranular phase (white regions in Fig. 2a). The above-described dendritic type microstructure is typical for as-cast alloys.

Fig. 2b presents the SEM image of the microstructure obtained after direct phase transformation in the $Nd_2Fe_{14}B$ alloy carried out in the hydrogen atmosphere of 0.1 MPa at transformation temperature of 730°C during 115 minutes in accordance with the kinetic data (Fig. 1a, curve 1). In this case, the decomposed alloy consists from the following main phases: α-phase of iron (dark regions in Fig. 2b) and NdH_2 phase (white regions in Fig. 2b). Because of this, comparison between microstructures of the decomposed (Fig. 2b) and initial (Fig. 2a) alloys shows that the decomposed alloy has a dendritic type structure too.

Then, in Fig. 2c, the SEM image of the $Nd_2Fe_{14}B$ alloy after 20 % of the reverse phase transformation (when the sample was treated in vacuum at transformation temperature of 730°C during 4.25 minutes, in accordance with the kinetic data in Fig. 1a, curve 2) is shown. As follows from this picture, the nucleation and growth of the new $Nd_2Fe_{14}B$ phase (grey regions in Fig. 2c) during the reverse phase transformation process starts at the NdH_2 phase (white regions in Fig. 2c). At first, the NdH_2 phase dissociates into Nd due to desorption of hydrogen and then Fe atoms diffuse to Nd and B atoms with formation of the new $Nd_2Fe_{14}B$ phase. Analogous mechanism has also been detected in similar $Nd_{16}Fe_{76}B_8$ alloy by TEM investigations [27].

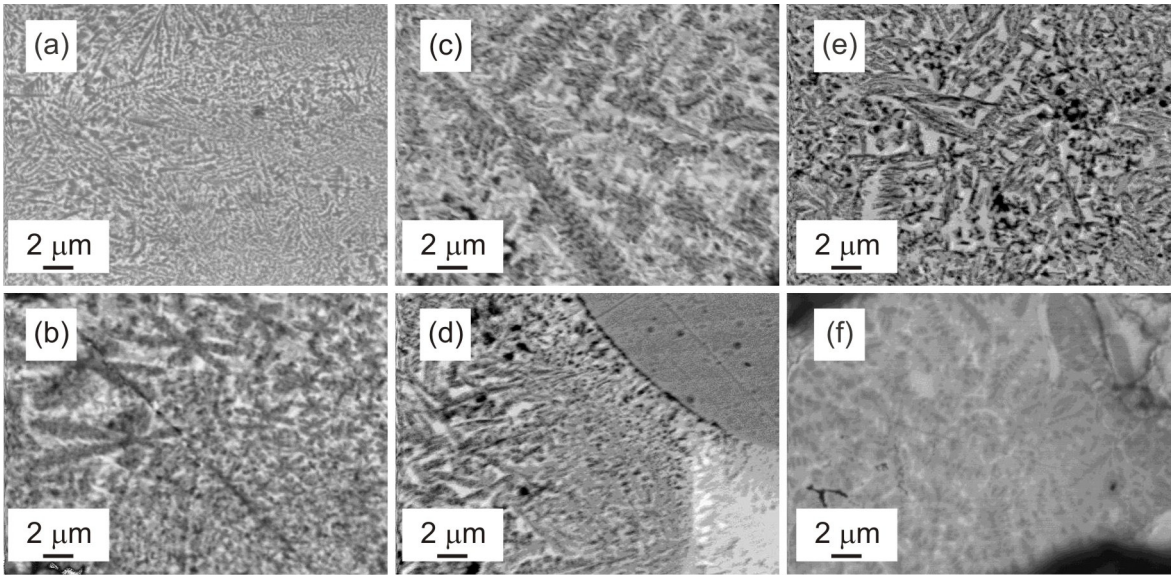

Fig. 2. (a) Scanning electron microscope (SEM) image of the initial $Nd_2Fe_{14}B$ alloy. (b) SEM image of the $Nd_2Fe_{14}B$ alloy after direct phase transformation (115 minutes). (c) SEM image of the $Nd_2Fe_{14}B$ alloy after 20 % of the reverse phase transformation (4.25 minutes). (d) SEM image of the $Nd_2Fe_{14}B$ alloy after 50% of the reverse phase transformation (10.0 minutes). (e) SEM image of the $Nd_2Fe_{14}B$ alloy after 80 % of the reverse phase transformation (23.5 minutes). (f) SEM image of the $Nd_2Fe_{14}B$ alloy after 100 % of the reverse phase transformation (95.0 minutes).

In Fig. 2d and 2e the SEM images of sample alloy after 50% of reverse phase transformation (10.0 minutes) and after 80% of reverse phase transformation (23.5 minutes), respectively, are presented. In Fig. 2f the image of the $Nd_2Fe_{14}B$ alloy after completion of the reverse hydrogen-induced phase transformation (at the same temperature of 730°C and vacuum ~1 Pa during 95 minutes that ensure a full completion of the reverse transformation according to data of Fig. 1a, curve 2) is shown. In this case $Nd_2Fe_{14}B$ alloy consists from $Nd_2Fe_{14}B$ hard magnetic Φ-phase (grey regions in Fig. 2f), Nd-rich intergranular phase (white regions in Fig. 2f) and with small amount of α-Fe phase (dark regions in Fig. 2f). As can be seen from Fig. 2f, microstructure of treated $Nd_2Fe_{14}B$ alloy has not dendritic structure type as in case of initial alloy (see Fig. 1a).

Then with goal more detailed studying of microstructure features further has been made high SEM studies of initial and final sample of $Nd_2Fe_{14}B$ alloy. In Fig. 3 are shown high scanning electron microscope (HSEM) image of initial $Nd_2Fe_{14}B$ alloy (Fig. 3a) and $Nd_2Fe_{14}B$ alloy after direct and reverse phase transformations (Fig. 3b) made at same conditions. As can be seen from HSEM image in Fig. 3a, microstructure of an initial $Nd_2Fe_{14}B$ alloy has dendritic structure.

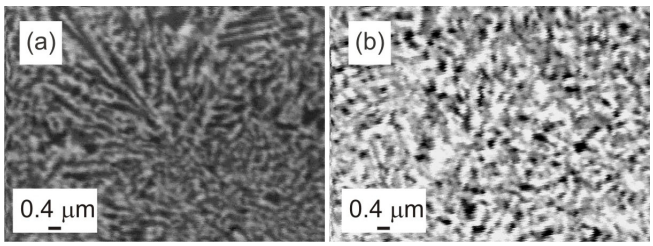

Fig. 3. (a) High scanning electron microscope (HSEM) image of initial $Nd_2Fe_{14}B$ alloy. (b) HSEM image of $Nd_2Fe_{14}B$ alloy after direct (115 minutes) and reverse phase transformations (95 minutes).

On the contrast, as follows from Fig. 3b, in case if hydrogen treatment is carried out by controlling of the transformation time in accordance with kinetic data for direct and reverse transformations in the $Nd_2Fe_{14}B$ alloy (Fig. 1a,b) it leads to transformation of initial dendritic structure type (Fig. 3a) into morphological ordered homogeneous nanocrystalline microstructure in $Nd_2Fe_{14}B$ alloy with fine grains of the main $Nd_2Fe_{14}B$ hard magnetic phase (grey regions in Fig. 3b) with average grains size ~0.3 μm. Because of thus, comparing microstructure presented in Fig. 3a and Fig. 3b shows that carrying out the direct and reverse phase transformations leads to decreasing of amount of a Fe phase (dark regions in Fig. 3) in $Nd_2Fe_{14}B$ alloy that is very positive factor for coecivity permanent magnets increase [28-30]. It's interesting that above-described microstructural results have good agreement with results in work [31] where similar microstructure was obtained in HDDR-treated $Nd_2Fe_{14}B$ type alloy with high coercivity by another way, i.e. by doping of Dy and Co elements to bulk alloy or alloying by Co, Zr and Ga elements [32]. Because of this, recently in work [33] also was obtained formation of morphological ordered homogeneous nanocrystalline microstructure in $Nd_2Fe_{14}B$ type alloy (with Ga and Nb elements addition to bulk alloy) by varying by one of main of kinetic parameters, i.e. changing of hydrogen pressure from 0.3 up to 1.0 bar during HDDR-treatment.

However, as an example, in some cases when some above-described HDDR schemes were applied to $Nd_2Fe_{14}B$ type alloys with various chemical composition it can lead to the abnormal grains growth processes of a hard magnetic $Nd_2Fe_{14}B$ Φ-phase up to tens-hundreds μm [25,34,35] and coercivity decrease.

From viewpoint of transformation kinetics there is explanation of processes of abnormal growth of $Nd_2Fe_{14}B$ hard magnetic phase. As it has been shown in our previous works [20-23] transformations of this type $Nd_2Fe_{14}B$ type alloys proceeds by mechanism of nucleation and growth. In case when direct hydrogen-induced phase transformation in $Nd_2Fe_{14}B$ alloy has been not completed decomposed alloy should consist from the following polyphase structure: undecomposed $Nd_2Fe_{14}B$ phase, α-phase of Fe, NdH_2 hydride phase and Fe_2B boride phase (see Eq. (1)). Further, at reverse transformation stage the undecomposed $Nd_2Fe_{14}B$ phases will be act as preferable site for nucleation of new $Nd_2Fe_{14}B$ phases that will be grow with very high speed in contrast to other ordinary $Nd_2Fe_{14}B$ centres. As a result, obtained microstructure should consist from many numbers of $Nd_2Fe_{14}B$ grains with small sizes and with not numerous large $Nd_2Fe_{14}B$ grains [25,34,35].

In the contrast with empirical approaches, hydrogen treatment of the $Nd_2Fe_{14}B$ alloys carried out by proposed scheme (Fig. 1b) in accordance with the isothermal kinetic data (Fig. 1a) allows to avoid abnormal grains growth processes and it also results in the microstructure formation corresponding to permanent magnets with high coercivity. This fact is a prerequisite for improving coercivity of permanent magnets [3,6,28-30] made of a nanocrystalline powder treated by this way.

Thus, proposed approach based on kinetic data of hydrogen-induced phase transformations in $Nd_2Fe_{14}B$ type alloys result in nanocrystalline microstructure formation that is necessary for permanent magnets with high coercivity without very complicated and expensive of alloying procedures.

4. Conclusions

SEM was applied to investigate the microstructure formation features during the hydrogen-induced transformations in the $Nd_2Fe_{14}B$ hard magnetic alloy. It is shown that the hydrogen treatment of the $Nd_2Fe_{14}B$ alloy, carried out in accordance with the isothermal kinetic data, leads to the formation of nanocrystaline microstructure.

On the base of the SEM microstructure studies it is established that process of nucleation and growth of the main magnetic $Nd_2Fe_{14}B$ phase during the reverse phase transformation starts near the NdH_2 hydride phase regions. After the completion of the reverse phase transformation, based on the kinetic transformation data, the $Nd_2Fe_{14}B$ alloy has morphological ordered homogeneous nanocrystalline microstructure with sub-micron grains having size of ~0.3 μm of the main $Nd_2Fe_{14}B$ hard magnetic phase.

In addition, if the treatment is carried out taking into account the hydrogen-induced transformation kinetic data, then the abnormal grains growth can be avoided in the $Nd_2Fe_{14}B$ alloy. The obtained results also may be considered as a base for the new method to produce nanocrystalline

powders of the $Nd_2Fe_{14}B$ type alloys for permanent magnets with improved magnetic properties.

References

1. R.W. Cahn, H. Kazuhiro, P. Haasen. Physical Metallurgy. North-Holland, New York, (1996) 2888 p.
2. J.W. Christian. The Theory Transformations in Metals and Alloys. Oxford, Pergamon Press, (2002) 1193 p.
3. J.M.D. Coey. Magnetism and Magnetic Materials. Cambridge University Press, Cambridge, (2010) 633 p.
4. Ya.M. Dovdalevskii. Alloying and thermal treatment of hard magnetic alloys. Metallurgiya, Moscow, (1971) 176 p. (in Russian).
5. I.B. Kekalo, B.A. Samarin. Physical metallurgy of a precision alloys: Alloys with special magnetic properties. Metallurgiya, Moscow, (1989) 496 p. (in Russian).
6. P. Campbell. Permanent magnet materials and their application. Cambridge University Press, Cambridge, (1994) 207 p.
7. M. Sagawa, S. Fujimura, N. Togawa et al. J. Appl. Phys. **55**, 2083 (1984).
8. J.J. Croat, J.F. Herbst, R.W. Lee, F.E. Pinkerton. J. Appl. Phys. **55**, 2078 (1984).
9. L. Schultz, J. Wecker, E. Hellstern. J. Appl. Phys. **61**, 3583 (1987).
10. R.W. Lee. Appl. Phys. Lett. **46**, 790 (1985).
11. H.H. Stademaier, N.C. Lui. Matter. Lett. **4**, 304 (1986).
12. C.R. Paik, H. Mino, M. Okada, H. Homma. IEEE Trans. Magn. **23**, 2512 (1987).
13. T. Takeshita, R. Nakayama. Proc. X Int. Workshop on Rare-Earth Magnets and Their Applications, Kyoto, Japan, 1989, pp. 551–558.
14. T. Takeshita, R. Nakayama. Proc. of the XI Int. Workshop on Rare-Earth Magnets and Their Applications, Pittsburg, USA, 1990, pp. 49–71.
15. T. Takeshita. J. Alloys Comp. **193**, 231 (1993).
16. O. Gutfleisch, I.R. Harris. Proc. XV Int. Workshop on Rare-Earth Magnets and Their Applications, Dresden, 1998, pp. 487–506.
17. R. Nakayama, T. Takeshita, M. Itakura, N. Kuwano, K. Oki. J. Appl. Phys. **76**, 412 (1994).
18. T. Takeshita, K. Morimoto. J. Appl. Phys. **79**, 5040 (1996).
19. T. Takeshita, R. Nakayama. IEEE Trans. J. Magn Japn. **8**, 692 (1993).
20. V.A. Goltsov, S.B. Rybalka, D. Fruchart, V.A. Didus. Kinetics and some general features of hydrogen-induced diffusive phase transformations in Nd2Fe14B type alloys. In: Progress in Hydrogen Treatment of Materials, ed. by Goltsov, V.A., Kassiopeya Ltd.–Coral Gables: Donetsk, Ukraine (2001) pp. 367–390.
21. S.B. Rybalka, V.A.Goltsov, V.A. Didus, D. Fruchart. J. Alloys Comp. **356**-**357**, 390 (2003).
22. V.A.Goltsov, S.B. Rybalka, A.F. Volkov, Yu.G. Putilov, V.A. Didus. The Physics of Metals and Metallography. **89**, 363 (2000).
23. V.A. Goltsov, S.B. Rybalka, A.F. Volkov. Functional Materials. **6**, 326 (1999).
24. T. Takeshita. J. Alloys Comp. **231**, 51 (1995).
25. I.R. Harris, P.J. McGuiness. Proc. XI Int. Workshop on Rare-Earth Magnets and Their Applications, Pittsburg, 1990, pp. 29–48.
26. O. Gutfleisch, A. Bollero, A. Kirchner, D. Hinz, et al. Annual Report Leibniz Institute for Solid State and Materials Research, Dresden, 2000, pp. 11–14.
27. O. Gutfliesch, M. Matzinger, J. Fidler, I.R. Harris. J. Magn. Magn. Mater. **147**, 320 (1995).
28. H. Kronmuller, K.-D. Durst. J. Magn. Magn. Mater. **74**, 291 (1988).
29. T. Weizhong, Z. Schuzeng, H. Bing. J. Magn. Magn. Mater. **94**, 67 (1991).
30. J. Fidler, T. Schrefl. J. Appl. Phys. **79**, 5029 (1996).
31. W. Chen, R.W. Gao, M.G. Zhu, W. Pan et. al. J. Magn. Magh. Mater. **261**, 222 (2003).
32. Y. Kawashita, N. Waki, T. Tayu, T. Sugiyama et. al. J. Magn. Magh. Mater. **269**, 293 (2004).
33. K. Guth, T.G. Woodcock, L. Schultz, O. Gutfleisch. Acta Mater. **59**, 2029 (2011).
34. E. Estevez, J. Fidler, C. Short, I.R. Harris. J. Phys. D: Appl. Phys. **29**, 951 (1996).
35. P.J. McGuiness, X.J. Zhang, K.G. Knoch et al. J. Magn. Magn. Mater. **104**-**107**, 1169 (1992).